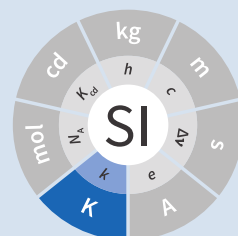


# Supplementary Information for the Realization of the PLTS-2000

1 édition 2014

October 29, 2014  
29 octobre 2014





**Supplementary Information for  
the Realization of the PLTS-2000**

**1<sup>st</sup> edition      2014**

---

29 October 2014

## Abstract

This document has been prepared by a task group of CCT Working Group 4 to give general guidance for establishing and measuring melting pressures of  $^3\text{He}$  in the range from 0.902 mK to 1 K, i.e. for realizing the PLTS-2000. It draws on published techniques and designs, and is intended to be suitable for application in national measurement institutes, as well as more generally in ultra-low temperature laboratories where absolute pressure standards are not normally available. It is a slightly modified version of the publication by Rusby *et al.* [2007].

The document describes methods by which the PLTS-2000 can be realized successfully. However, it should not be taken as laying down how it must be done. The description of any particular apparatus is more for illustration than prescription, and considerable variation can often be effective. Likewise, quoted numerical data and dimensions are mostly for guidance only.

# 1. Introduction

The Provisional Low Temperature Scale of 2000, PLTS-2000, was adopted by the CIPM in October 2000 to provide an extension of the International Temperature Scale of 1990, ITS-90, to lower temperatures. It ranges from the Néel temperature of solid  $^3\text{He}$ ,  $T_{2000} = 0.902 \text{ mK}$ , up to 1 K, thus overlapping the ITS-90 between 0.65 K and 1 K. The definition and derivation of the PLTS-2000 has been published by Rusby *et al.* [2002].

The requirements of temperature measurement in the range well below 1 K differ from those at higher temperatures in nature as well as in degree. There are no longer any gases whose properties can be used in gas thermometry (for primary measurements or interpolation) or in vapour pressure thermometers (as used in the ITS-90). Thermal radiation is virtually extinct, and thermometry must rely mainly on the electrical, magnetic or nuclear properties of condensed matter, whose characteristic energies lie in the millikelvin range. Moreover, the rapid increase in thermal resistances on cooling means that measurements must be almost non-dissipative.

In spite of this, a surprising variety of thermometers have been exploited to meet needs in various parts of the range and with varying degrees of linkage to thermodynamics or statistical physics [Hudson *et al.* 1975, Schuster *et al.* 1994, Lounasmaa 1974, Betts 1976, Richardson and Smith 1988, Pobell 1996]. Examples are: noise thermometry using SQUIDs; paramagnetic (Curie law) susceptibility of dilute salts, magnetic alloys or nuclear spins; NMR; anisotropy of gamma-ray emissions to probe the population of hyperfine spin-states in radioactive nuclei; second-sound or osmotic pressure in  $^3\text{He}$ - $^4\text{He}$  mixtures; viscometry using vibrating wires; and  $I$ - $V$  characteristics of junctions between metals, semiconductors and superconductors; and in addition the secondary (e.g. resistance) thermometers which may be calibrated against them.

These thermometers all have their advantages and disadvantages, but none has all the qualities necessary for defining an International Temperature Scale—sensitivity, reproducibility, practicality (convenience of realization or calibration), and universality. Noise thermometers, which may operate in a primary or secondary way over the whole range, suffer from potential offsets which must be taken into account. The CMN magnetic thermometer has materials-related difficulties due to purity and poor thermal diffusivity in single crystals, or ambiguities over the Weiss constant in a powdered sample. Most other thermometers are only suitable as secondary devices, and the ranges of usefulness of many are limited, so that more than one would be needed to construct a complete scale.

However, a thermometer using the melting pressure of  $^3\text{He}$ , which was first proposed by Scribner and Adams [1970], almost entirely meets the requirements. In 1996, the CCT called for a  $^3\text{He}$  melting-pressure equation to be derived to serve as the basis for an extension of the ITS-90 down to a temperature of about 1 mK, analogous to the use of the vapour pressures of  $^3\text{He}$  and  $^4\text{He}$  in the ITS-90.  $^3\text{He}$  is a well-defined substance, with sufficient availability, and the melting pressure,  $p_m$ , is sensitive to temperature over most of the range of interest. However, there were differences of opinion regarding the  $p_m - T$  relationship at the lowest temperatures, at the level of  $\pm 2\%$  of  $T$ , and as a result the PLTS-2000 was adopted on a provisional basis only. These differences have not yet been resolved.

The equation adopted for the melting pressure  $p_m$  in the PLTS-2000 is

$$p_m / \text{MPa} = \sum_{i=-3}^{+9} a_i (T_{2000} / \text{K})^i, \quad (1)$$

with the following coefficients:

$$a_{-3} = -1.3855442 \cdot 10^{-12}$$

$$a_{-2} = 4.5557026 \cdot 10^{-9}$$

$$a_{-1} = -6.4430869 \cdot 10^{-6}$$

$$a_0 = 3.4467434 \cdot 10^0$$

$$a_1 = -4.4176438 \cdot 10^0$$

$$a_2 = 1.5417437 \cdot 10^1$$

$$a_3 = -3.5789853 \cdot 10^1$$

$$a_4 = 7.1499125 \cdot 10^1$$

$$a_5 = -1.0414379 \cdot 10^2$$

$$a_6 = 1.0518538 \cdot 10^2$$

$$a_7 = -6.9443767 \cdot 10^1$$

$$a_8 = 2.6833087 \cdot 10^1$$

$$a_9 = -4.5875709 \cdot 10^0.$$

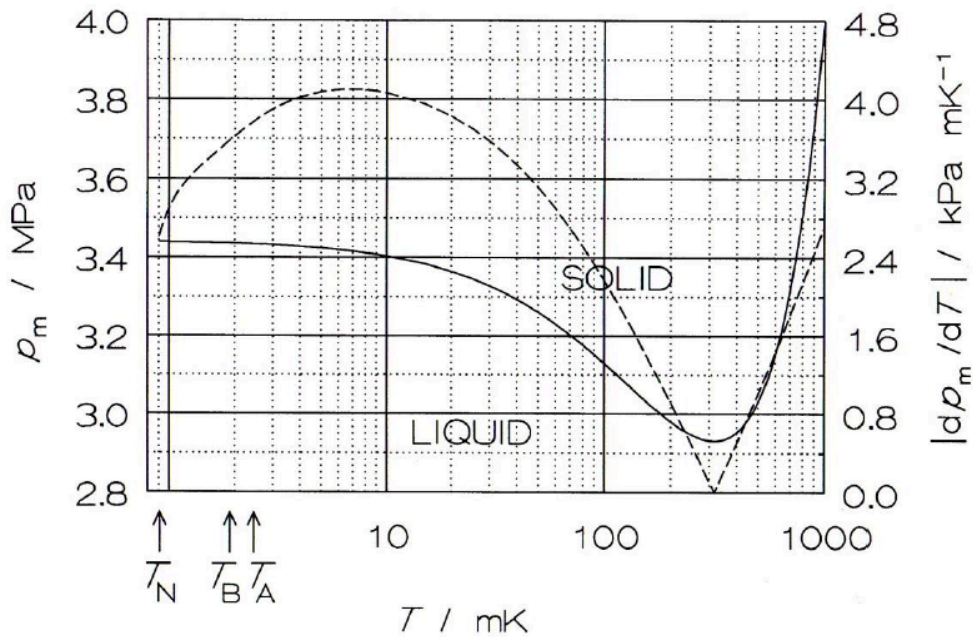


**Figure 1 — The  $^3\text{He}$  melting pressure,  $p_m$ , (full line) and the absolute value of the derivative  $dp_m/dT$  (dashed line, right-hand scale) versus temperature, from [Durieux and Reesink 1999].  $T_N$ ,  $T_B$  and  $T_A$  indicate the temperatures of three phase transitions in solid or liquid  $^3\text{He}$ .**

Figure 1 is a graphical representation of the melting curve below 1 K, which shows that the pressure range of interest is from 2.93 MPa to 4.0 MPa. Values of  $p_m$  and  $dp_m/dT_{2000}$  are tabulated at intervals of  $T_{2000}$  in Annex 1.

The melting pressure of  $^3\text{He}$  was chosen as the property on which the scale should be based because of the sensitivity and reliability with which it may be measured over a wide range, covering more than three decades of temperature, apart from a narrow region around the pressure minimum, at  $T_{\text{min}} = 315.24 \text{ mK}$ . It is a thermodynamic property with few complications arising from purity, *etc.*, it provides an unambiguous universal definition, and it is capable of being realized in laboratories around the world without the exchange of artifacts.

However, there are also some practical complications. In particular, the melting-pressure cell must operate at high pressure, with implications for the cell design and gas-handling system, and it must include a pressure transducer capable of good sensitivity and reproducibility.

## 2. Requirements and features

Fundamentally the operation of a melting pressure thermometer (MPT) requires that a sample of pure liquid and solid  $^3\text{He}$  be brought to equilibrium at the desired temperature, and that the equilibrium pressure be measured absolutely. Following the original work of Straty and Adams [1969], several designs of MPT have been described; see for example [Greywall and Busch 1982, Bremer and Durieux 1992, Schuster *et al.* 2001]. In what follows particular use is made of three publications, due to Schuster, Hoffmann and Hechtfischer [2001]; Colwell, Fogle and Soulen [1992], who used a thermometer provided by Greywall [1982]; and Adams [2005]. They are here designated SHH, CFS and EDA, respectively.

A consequence of the inversion in pressure is that for temperatures below  $T_{\min}$  the cell cannot communicate at constant pressure with an external measuring system: the sensing capillary is blocked with a plug of solid  $^3\text{He}$ , and direct contact with the pressure in the cell is lost. A melting-pressure cell must therefore include a pressure transducer, and this leads to the particular usefulness of the intrinsic fixed points discussed below.

In the region around the minimum the thermometer cannot be used directly and some interpolation is required. The method for doing this is not specified in the PLTS-2000, but it can use any secondary sensor (CMN, resistive, etc.) which can be calibrated in this range. Although it may be surprising to base a scale on a thermometer where there is a region of low or zero sensitivity, the minimum has the compensating advantage of providing an in-built pressure fixed point which can be used for the calibration of the pressure transducer, as will be seen. SHH show that by stepping carefully through the minimum, the temperature can also be located, within about  $10\ \mu\text{K}$ .

Figure 1 indicates the three other intrinsic fixed points of pressure and temperature, which may be detected and used as fixed points of pressure and temperature for the in situ calibration of the pressure transducer. They are the transition to the superfluid ‘A’ phase, the ‘A to B’ transition in the superfluid and the Néel transition in the solid. The pressure and temperature values of the four fixed points on the PLTS-2000 are shown in Table 1, with the estimated thermodynamic uncertainty (at  $k = 1$ ) in the temperatures,  $T$ , and the uncertainty of the current best practical realization of each point,  $\delta T_r$ . For the three low-temperature features,  $\delta T_r$  comes from the pressure resolution with which they can be observed (about  $\pm 3\ \text{Pa}$  for  $p_A$  and  $p_{\text{Néel}}$ ,  $\pm 10\ \text{Pa}$  for  $p_{A-B}$ , see Chapter 5, see p. 17) coupled with the derivative  $dp_m/dT$ . For the minimum, the pressure resolution is also about  $\pm 3\ \text{Pa}$ ;  $\delta T_r$  comes from locating the point of zero derivative in SHH. The uncertainty in the assigned absolute pressure values was estimated by [Rusby *et al.* 2002] to be  $\pm 60\ \text{Pa}$ .

**Table 1.** Values of  $p_m$  and  $T_{2000}$  for the  $^3\text{He}$  melting-pressure features, with estimated standard uncertainties with respect to thermodynamic temperature,  $T$ , and the standard uncertainties of the current best realizations,  $\delta T_r$ .

Point	$p_m / \text{MPa}$	$T_{2000} / \text{mK}$	$\Delta T / \mu\text{K}$	$\delta T_r / \mu\text{K}$
Minimum	2.931 13	315.24	360	10
A	3.434 07	2.444	48	0.7
A-B	3.436 09	1.896	38	2.8



Point	$p_{\text{m}}/\text{MPa}$	$T_{2000}/\text{mK}$	$\Delta T/\mu\text{K}$	$\delta T_{\text{r}}/\mu\text{K}$
Néel	3.439 34	0.902	18	1.1

### 3. Cell design

In practical realizations the pressure transducer relies on the capacitive sensing of the displacement of a diaphragm in the cell. The interior, which is typically only a few  $\times 100\text{mm}$  in volume, contains a sinter, usually of silver powder, to promote thermal contact with the liquid  $^3\text{He}$  and reduce the time constant for equilibrium. Two examples are shown in Figure 2, in which a parallel-plate capacitor senses the displacement of the diaphragm.

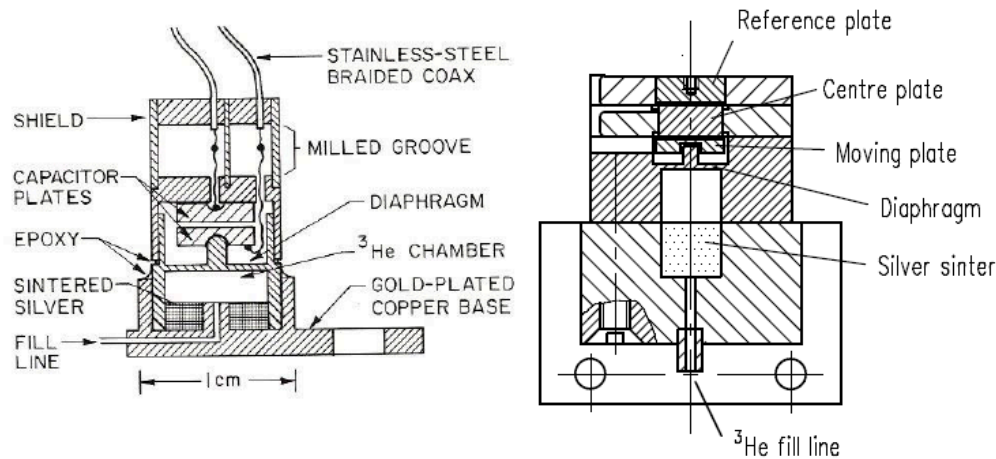


**Figure 2 —  $^3\text{He}$  melting-pressure cells of Greywall and Busch [1982] (diaphragm of coin silver, diameter 6.4 mm, thickness 0.25 mm) and SHH [Schuster *et al.* 2001] (diaphragm of BeCu, diameter 6.1 mm, thickness 0.4 mm).**

The design, construction, methods of measurement, and uses of high-resolution capacitive pressure gauges in low-temperature applications have been reviewed by Adams [1993]. The most critical design parameters of the transducer are the diameter and thickness of the diaphragm, which is usually made of coin silver or BeCu, and the parallelism of the capacitance plates in order to achieve the desired sensitivity, linearity and reproducibility of the device. Considerable care must be taken to ensure that the capacitance plates are parallel, and that the gap is small so as to achieve good sensitivity. For example, Greywall and Busch allowed the epoxy on the lower plate and the top cap to cure while the plates were in contact and the cell was at 4.4 MPa pressure. When the pressure was relieved, they estimated that the spacing between the plates was  $36\text{ }\mu\text{m}$ . SHH, whose diaphragm was rather thicker, used  $10\text{ }\mu\text{m}$  and  $7\text{ }\mu\text{m}$  foils to set the spacings during the curing of the epoxy on the moving and reference plates, respectively.

An alternative cell uses the distension of the cylinder walls in a co-axial capacitor. This was first used in measurements with solid  $^4\text{He}$  [Jarvis *et al.* 1968], and it has also been applied to melting-pressure thermometry [Mikheev *et al.* 1994].

## 4. Installation and procedure

In operation the cell is bolted to the experimental platform where the temperature is to be measured. External thermal contact is thus metal-to-metal, ideally gold plated, and within the cell heat transfer from the cell body to the  $^3\text{He}$  is mainly between the liquid and the sinter. The filling and sensing line is generally a copper-nickel capillary of about 0.5 mm diameter which is soft-soldered to a bush on the cell. It is thermally anchored at several points in the refrigerator to reduce heat conduction and to permit calculation of the hydrostatic head correction for absolute pressure calibration (see below). From 4.2 K up to room temperature the tube may be wider, up to 1 mm diameter, and in a vacuum jacket to insulate it from the liquid helium and temperature variations during helium fills. It is advisable to include a second tube to act as an emergency outlet should the first become blocked with impurity such as solid air. SHH include a filter at 1.5 K to keep the system free of solid particles, and they describe their method for anchoring the capillary at 1.5 K, at the still (0.5 K), the base plate (0.06 K), and at the mixing chamber. Finally they describe how the capillary is connected to the melting-pressure cell.

Since pure  $^3\text{He}$  is expensive and is only available in small quantities, the sample of typically 0.5 mol is kept in a small storage cylinder to which it is returned after use. SHH recommend that the cylinder should be 20 L so that storage is always well below ambient pressure, to guard against loss. The gas can otherwise be stored at some convenient elevated pressure.

The cylinder is connected to the gas-handling system through a valve so it can be removed or replaced. The other essential components of the gas handling are a liquid-nitrogen-cooled ‘dipstick’ sorption cleaner to remove air and other condensable gases, a  $^4\text{He}$ -cooled dipstick to absorb the sample and generate the necessary high pressures, low and high pressure adjustable valves and gauges, as well as connections to the pressure measuring system and vacuum pumps. Both EDA and SHH give details of their systems, and that of EDA is illustrated in Figure 3 (see [Adams 2005] for a full description). SHH describe two versions, one which provides the essential features and another which is more versatile and allows for external pressure calibration and measurement.

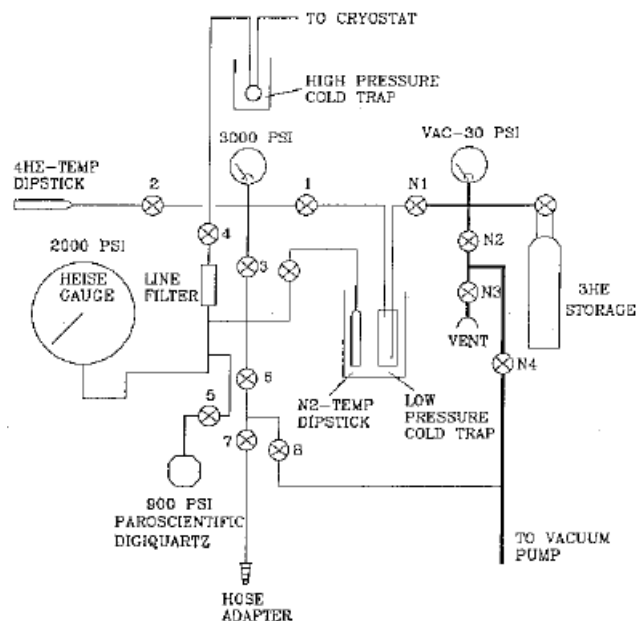


Figure 3 — The  $^3\text{He}$  gas-handling system of Adams [2005].

The procedure for condensing the sample in the cell at high pressures is typically as follows. The gas is passed through a charcoal sorption trap or dipstick at liquid-nitrogen temperature to ensure that any air or other impurity gases are removed from it. It is then absorbed in the  $^4\text{He}$  dipstick at 4.2 K, which is capable of holding the required quantity of gas and of withstanding the high pressures when it is released into the cell. SHH use a low-pressure dipstick in both nitrogen and helium to remove impurities, and an additional high-pressure helium dipstick.

The cell is first evacuated at room temperature using the helium-cooled trap, allowing sufficient time for gas to migrate along the fine capillaries. The system may also be flushed with gas to ensure that there are no blockages. The cryostat is then cooled to 4.2 K (SHH), or lower (CFS, EDA), whereupon the cell is ready to receive the gas. This is admitted by slowly raising the dipstick in the vessel of liquid helium with the valve to one of the capillaries open, monitoring the pressure on a convenient gauge. It is advisable to fill to progressively higher pressures in steps of 0.5 MPa (SHH), recharging the dipstick if necessary and checking the functioning of the pressure transducer at each stage, until the maximum operating pressure is reached (3.5 MPa for temperatures below 0.8 K, 4 MPa for measurements up to 1 K).

After condensing the gas at about 1.2 K the transducer should be ‘trained’ and calibrated. Training consists of cycling the pressure over the intended range of use, so as to improve its repeatability. SHH recommend 10 cycles for the full range 2.9 MPa to 4 MPa. Subsequently calibration takes place by reading the capacitance bridge at a series of known pressures. These are generated by a pressure balance (CFS) or they are measured using a calibrated secondary gauge, such as a quartz oscillator gauge (SHH, EDA). Again it is advisable to check the repeatability of the calibration data in more than one pressure cycle.

The uncertainty of the reference pressures clearly affects the overall uncertainty which can be achieved, but another factor is the need to correct for the hydrostatic pressure head due to the  $^3\text{He}$  liquid (and vapour) in the capillary: the value of the pressure head is typically about 650 Pa to 700 Pa (SHH, CFS), and the uncertainties in its determination are likely to be significant. However, it is possible to reduce the uncertainties, or avoid the need for external calibration altogether, by using the intrinsic fixed points of  $^3\text{He}$ . The various options are discussed later.

The melting-pressure thermometer is now set up and available for use, except that no solid has yet been formed. This occurs only when the cell is cooled to the melting curve, whereupon solid preferentially forms in the open volume of the cell, leaving the liquid to maintain good thermal contact through the silver sinter. The initial condition for the formation of the solid must be carefully chosen, as there is no single starting point which allows a complete realization to be achieved; *i.e.*, for liquid and solid to coexist throughout the range 0.9 mK to 1 K. Thus a sample of 100 % liquid at 1 K and 4 MPa becomes 100 % solid at 0.55 K. In practice it may take several attempts to achieve the desired conditions, because the volume and temperature profile of the filling line influences the pressure at which the melting curve is reached.

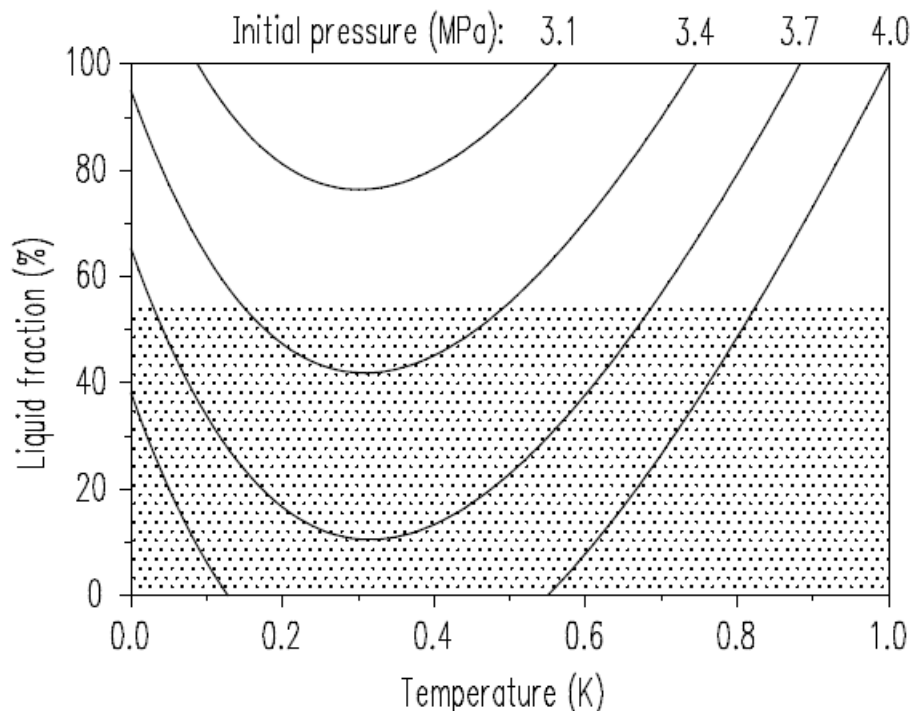


**Figure 4 — Co-existence curves of solid and liquid  $^3\text{He}$ , expressed as liquid fraction, for four different initial pressures, SHH (Figure 13). The dotted area shows that about 55 % of the volume of the SHH cell contains sinter, and hence indicates the temperature ranges over which this is penetrated by solid  $^3\text{He}$ .**

Figure 4, from SHH, shows a family of curves indicating how the range of use varies with the pressure at which solid is initially formed. For example, a sample initially at 3.7 MPa could in principle be used from 0.88 K to 0.9 mK, but for most of the range solid would penetrate the sinter, leading to erroneous results, see below. On the other hand, a sample initially at 3.1 MPa is suitable for observing the minimum, but the range of use is only 0.56 K to about 0.1 K.

EDA illustrates the requirements for the filling pressure by reference to a plot of the molar volumes of liquid and solid, Figure 5, the two-phase region being between the two curves. Once the plug has formed, the sample follows a horizontal path, at constant molar volume: at any point in the two-phase region, the relative distance from the two curves indicates the proportion of solid to liquid in the cell. Clearly, too high a starting pressure, *i.e.* too low a molar volume, results in too much solid being formed.

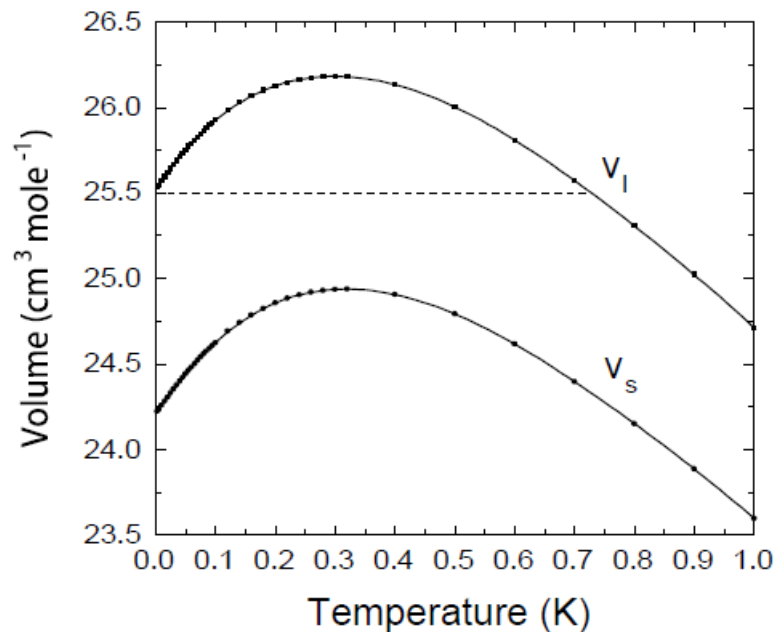


**Figure 5 — Molar volumes of liquid and solid  $^3\text{He}$  at the melting pressure, with the region of co-existence lying between the two curves, from Adams [2005]. The horizontal dotted line indicates the path taken by the sample if the plug is formed at 3.38 MPa.**

SHH and EDA both note that a filling pressure of about 3.37 MPa (which generates solid below 0.73 K) can be used to observe the minimum correctly and also the low temperature fixed points, but this can only be done if the open volume of the cell is 55 % or more. In practice they prefer to have more sinter, in order to ensure good contact between the liquid and the cell, and hence good response at the lowest temperatures. In this case a lower-pressure filling is needed to observe the minimum, after which the pressure is reset at the higher value for operation at lower temperatures.

The melting pressure of helium in confined geometries is higher than in the bulk<sup>20</sup>, with the result that when the open volume becomes completely full of solid, on further cooling the pressure no longer follows the melting curve but remains approximately constant, and the temperatures calculated from the thermometer are anomalously high. An example of the effect of solid penetration into the sinter is shown in Figure 6, from SHH. Starting from about 1 K, the cell followed the melting curve down to about 0.75 K, after which it deviated strongly because the open volume was full of solid. Thereafter the temperature deviations steadily increased until just below 0.6 K, when even the sinter volume was full of solid and there was no longer a melting transition.

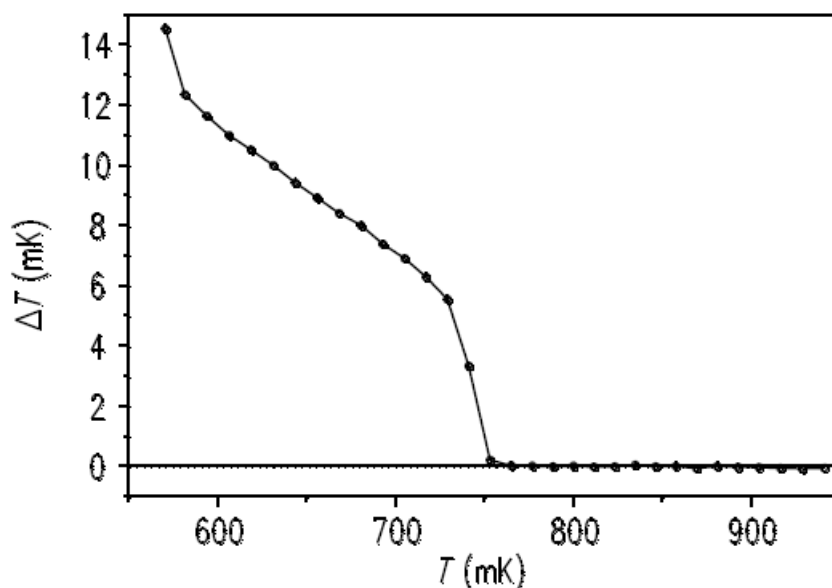


**Figure 6 — Example of temperature deviations when solid  $^3\text{He}$  is forced to grow into the sinter, from SHH (Figure 14).  $T$  is the difference between the indications of the melting pressure sensor and a reference thermometer on the cell, during cool-down.**

The formation of the plug of solid  $^3\text{He}$  in the filling capillary, which isolates the cell from the external system, also has other implications for procedure. Once the chosen initial pressure has been set, it is essential that no more  $^3\text{He}$  enters the cell, or extra solid will form. Therefore some point on the capillary should be colder than the cell (above the minimum) or warmer than the cell (below the minimum). Neither condition is difficult to achieve (see, for example, EDA), but ‘plug slip’ can be a problem in traversing the minimum. Unwanted growth of the solid should not be excessive if the initial pressure was low enough and the capillary inlet valve is kept closed, in which case repeated cooling and warming through the minimum should lead to repeatable behaviour.

Figure 7 shows pressure traces as the SHH cell is taken through the minimum and back again in steps of 0.5 mK, after correct and incorrect filling. The authors state that ‘any weak, sluggish or asymmetric response’ indicates that there is solid in the sinter leading to a high melting pressure.

A series of more rapid passes through the minimum over a period of 19 hours showed evidence of modest drift in  $p_{\min}$ , at an acceptable level of 3 Pa. This is ascribed to redistribution of solid in the sample, which also occurs after any change in temperature. In general, thermal problems in the operation of the melting-pressure sensor are indicated by poor response and long equilibration times at a steady temperature.

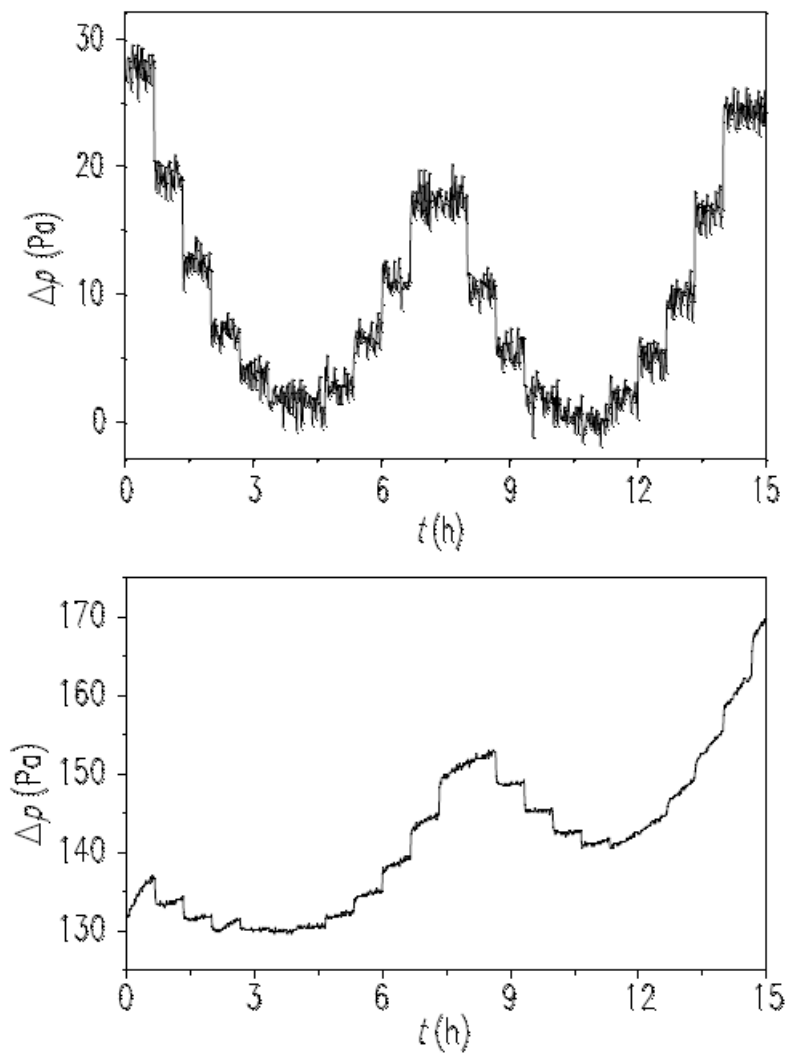


**Figure 7 — Realizations of the melting pressure minimum with correct (above) and incorrect (below) initial pressures, from SHH (Figure 15).**



## 5. Pressure and capacitance measurement

Conventionally the melting-pressure transducer is calibrated relative to an external reference standard, such as a pressure balance or a gauge with a traceable calibration. Since the transducer is not repeatable on cycling to low temperatures, this must be done on each cool-down, and corrections must be applied for the significant pressure gradients; *i.e.* for the hydrostatic pressure head of liquid and gaseous  $^3\text{He}$  in the capillary. The purpose of the calibration is to determine the relationship between the measured capacitance,  $C$ , and the pressure,  $p$ . This should be approximately linear with  $(1/C)$ , but in practice SHH and CFS use least-squares fits of the form  $p = f(1/C)$ , with two or more terms to allow for non-linearities.

The fundamental approach is to use the pressure balance or gauge to measure the pressures absolutely throughout the range, making corrections for the hydrostatic head in the capillary. This was done by CFS and SHH, and others, in the experiments which led to the derivation of the PLTS-2000.

However, for a *realization* of the PLTS-2000 use is made of the  $^3\text{He}$  features, as specified, to simplify the calibration. In particular, normalizing the calibration to the pressure minimum avoids the need to evaluate the hydrostatic head. If the features at lower temperatures can also be reached, then the pressure measurement in the range 2.93 MPa to 3.43 MPa is essentially an interpolation, and only non-linearities need be assessed. The various options are discussed below.

A detailed description of the use of a pressure balance (piston gauge) is beyond the scope of this document. It suffices to say that the balance is used to generate pressures according to the ratio of the weight of the loaded piston to its cross-sectional area (the axis being vertical). The pressures may be constant and repeatable to about 1 part in  $10^6$ , and uncertain, with a traceable calibration at the highest level, to about 1 part in  $10^5$ . Uncertainties in the weights used should be significantly smaller. The generated pressure can communicate directly with the sample in the cell, above the minimum, provided that the  $^3\text{He}$  is used as the working gas in the balance and the inevitable gradual loss of gas through the piston-cylinder assembly is accepted. This was the method adopted by CFS. Otherwise an oil-lubricated pressure balance may be used [Bremer 1992], or a differential gauge (such as a capacitance diaphragm gauge) can be used to separate the sample and the balance, but with additional complexities and uncertainties. The calibration process requires a series of pressures to be generated in the range of interest, by changing the load, and associating them with the corresponding capacitances of the transducer.

To avoid the possible contamination of the  $^3\text{He}$  sample, SHH preferred a two-stage process in which a secondary quartz-oscillator pressure gauge was first calibrated against a pressure balance, and then used to calibrate the melting-pressure transducer. Pitre *et al.* [2003] followed a similar procedure, and EDA also used a calibrated quartz-oscillator transducer (see below). The pressure must be held steady during the calibration and this can be done by controlling the temperature of the cell on the melting curve itself, above the minimum. However, it is usually more convenient to carry out the complete calibration while the cell is at a steady temperature near 1.2 K, adjusting and regulating the pressure rather than the temperature.

SHH have used this technique, and describe an additional cryogenic pressure-control cell which can be connected in the sensing line to act as a small  $^3\text{He}$  buffer volume. By varying the temperature of this cell, pressure variations over a range of 50 kPa can be induced, sufficient for control purposes. With the quartz-oscillator pressure gauge in the control loop, the residual pressure fluctuations remain below 10 Pa. Ihas and Pobell [1974] describe a similar system, and EDA suggests observing the output of the quartz gauge and manually adjusting the

external pressure while the readings are taken. Pitre *et al.* found that if the flow impedance between the cell and the pressure gauge is small and the conditions are steady enough, there was no need to actively control the pressure, even though normal changes occurred along the filling line and at room temperature.

As noted earlier, an ideal transducer would have a linear response to pressure, but in practice this is only approximately observed. Figure 8 shows the deviations from linearity which SHH found for five transducers in the range 2.93 MPa to 3.43 MPa (*i.e.* for the temperature range up to 0.76 K). In all but one case the maximum effect is equivalent to less than 0.1 mK, and all were well-fitted by quadratic equations. Bremer [1992] found a similar behaviour, but with a somewhat larger amplitude over this range. Pitre *et al.*, who used a PTB sensor, preferred a cubic fit but do not state the non-linearity.

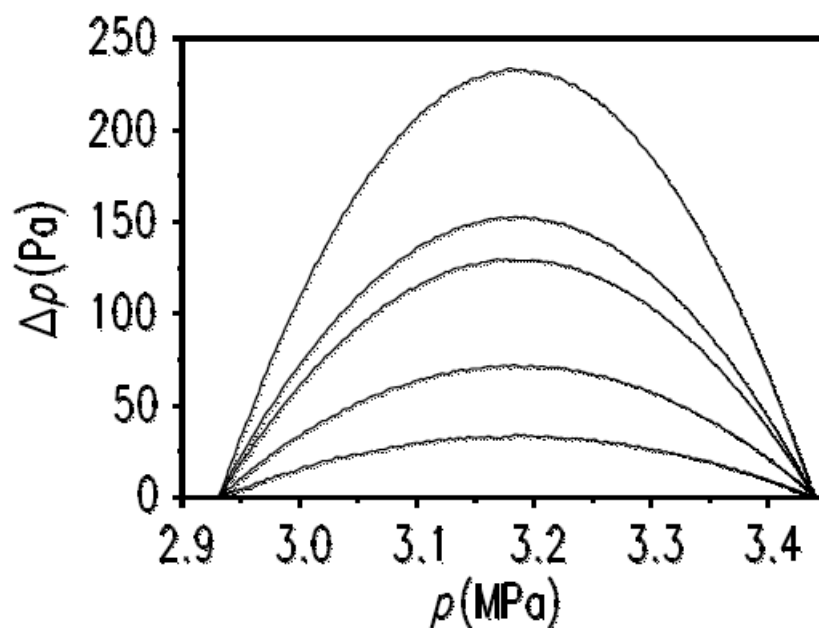


**Figure 8 — Non-linearity of five melting-pressure transducers, from SHH (Figure 21).**

A further effect is hysteresis in the transducer. SHH show this for one of their sensors, see Figure 9. The effect clearly depends on the pressure range covered, being  $\pm 100$  Pa for the full range, 2.93 MPa to 4 MPa, but only about  $\pm 20$  Pa for the range up to 3.43 MPa. The latter is hardly significant, but it is desirable to train the transducer in the range over which it is to be used. If necessary, for the wider range, the effect could be mitigated by using different calibrations for increasing and decreasing pressures.

SHH note that, in contrast to the calibration itself, the non-linearity and hysteresis of a transducer are repeatable after cycling to room temperature and back, and therefore that two points may be sufficient for a recalibration. However, Pitre *et al.* found a hysteresis in the first run they report of about 0.16 mK (330 Pa) at 0.78 K, but no hysteresis was detected in later runs. All new sensors must be fully investigated.

It is also necessary to check that the calibration of the transducer is independent of temperature. This can be done by cooling the cell at a constant pressure, below  $p_{\min}$ , and observing any changes in output. SHH found that the effect in their transducer was less than  $\pm 20$  Pa.

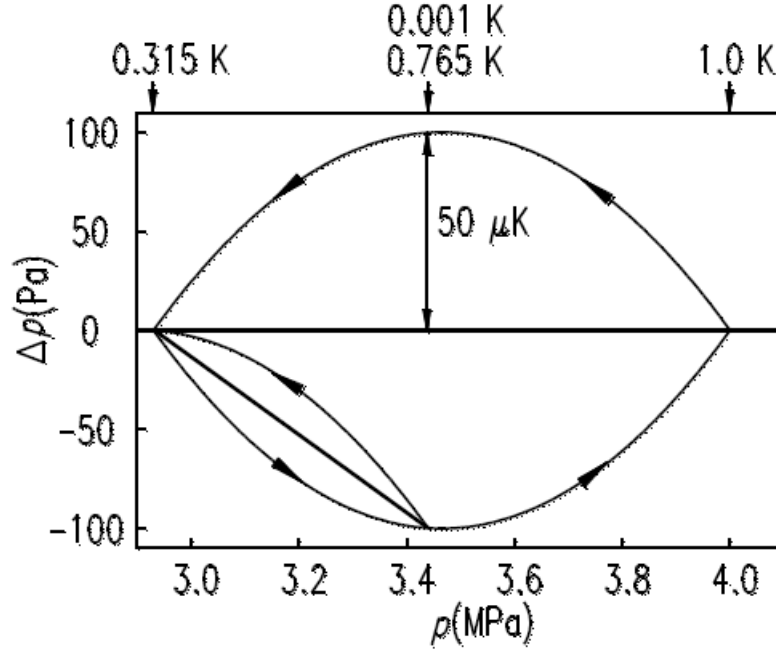


**Figure 9 — Pressure deviations due to sensor hysteresis, from SHH (Figure 22).**

Both CFS and SHH made corrections for the hydrostatic pressure head, and these are the experiments which led to the absolute determinations of  $p_{\min}$  in deriving the PLTS-2000. The authors describe their systems, and the method of determining the correction. Essentially this requires knowledge of the temperature profile along the capillary, in order to integrate the density of the fluid over the vertical head. CFS refer to Appendix 10 of Reference 24 for the density in the liquid phase and Bogayavlenskii *et al.* [1978] for the vapour phase. To simplify the calculation, in both experiments the temperature was arranged to be constant along vertical sections of the capillary. In both cryostats the magnitude of the correction was in the region of 650 Pa to 770 Pa, and the uncertainties were approximately 10 Pa (CFS, SHH, see also [Fellmuth 2003]). There is in addition a small pressure dependence amounting to about 25 Pa between 2.9 MPa and 3.4 MPa, *i.e.* about 0.01 mK (1 % of T) at 1 mK (SHH).

In principle, all measurements of the pressure using external references must take account of the hydrostatic pressure head, but for a realization of the PLTS-2000, it is sufficient (in fact necessary) to normalize the pressure to the specified value at the minimum and, if possible, at one of the other feature temperatures. In so doing, the need for a hydrostatic head correction can be avoided.

If the  $^3\text{He}$  superfluid or Néel temperatures can be reached (which requires a nuclear cooling stage), the given pressure values can be used to fix the calibration near 3.4 MPa, and the transducer is then essentially a pressure interpolation device, required only to be linear (see above). For operation in this range, normalization at one of these features is highly desirable, and EDA recommends  $T_N$ , for practical reasons. It can be observed as a distinct change in the derivative  $dp_m/dT$ , which is sharp enough to locate the transition precisely. A slight difference between the point seen on warming and cooling may limit the precision to about  $\pm 3$  Pa. The A-transition is second-order with a significant step-increase in heat capacity below  $T_A$ . It can be detected dynamically as a change in pressure drift rate as the temperature sweeps through the transition at a constant rate, either warming or cooling. A compromise has to be made between detectability and the rate of sweep, but SHH find that a detection uncertainty of this transition can also be  $\pm 3$  Pa. By contrast, the A-B transition is first-order with an undercool

such that it can only be reliably detected on warming, and it is less suitable for use as a fixed point.

If these points are not accessible, a superconductive transition temperature can be used, for example that of tungsten near 15 mK (where the melting pressure is about 3.38 MPa). Other possibilities are beryllium (23 mK, 3.35 MPa), or iridium (99 mK, 3.13 MPa), though the latter pressure is rather close to the minimum. At higher temperatures the transitions in cadmium (0.52 K, 3.06 MPa) or, more usefully, zinc (0.85 K, 3.62 MPa) or molybdenum (0.92 K, 3.79 MPa) can be used, or a calibration can be carried out using a sensor traceable to the ITS-90 (but see Chapter 7, see p. 24). Defined transition temperatures have not been established because of variations between samples, and each sample must therefore be individually calibrated. Hence this method involves traceability to an external source.

The capacitance of the transducer is generally measured by ratio to a reference capacitor which may either be within a bridge, or in an external temperature-stabilized enclosure (CFS), or in the cryostat (EDA). In the latter case it can be constructed as part of the cell (SHH), which gives the advantage of similarity of the connections to the sensing and reference capacitors. An alternative technique is to use resonance detection in an LC oscillator [Adams 1993, Van Degrieff 1975].

The SHH capacitance ranged from 23 pF to 40 pF, with a sensitivity of about  $5 \text{ pFMPa}^{-1}$ , and their three-terminal bridge was operated at 0.5 V and 175 Hz, which gave a heat load of 0.2 nW. The measurement scatter, integrated over 1 minute, was about  $0.3 \mu\text{K}$ . SHH conducted trials of various voltage and frequency excitations, and connection options, and selected an arrangement which gave self-heating of less than  $0.14 \mu\text{K}$  at the lowest temperatures. This was then applied throughout the range, to avoid corrections due to the voltage dependence of the dielectric materials.

CFS balanced the voltage across the capacitor against that of a 100 pF reference capacitor using a ratio transformer. At  $2 \text{ V}_{\text{rms}}$  and 1392 Hz excitation the sensitivity was 1 part in  $10^6$ , and no apparent heating of the melting pressure sensor was detected in their experiments down to 7 mK. EDA emphasizes the need to use 3-terminal connection to the cell capacitor because the resolution required is small compared with the capacitance of the coaxial connecting lines: each plate of the capacitor is connected to a separate coaxial line, with the third terminal being the ground. If the reference capacitor is mounted on the cell, the third coax line goes to the common plate.

Further details of the measurement and connection techniques are given in several references, *e.g.* [Mikheev *et al.* 1994, Schuster and Wolber 1986]. Clearly the performance of the bridge, and the design and pressure sensitivity of the capacitor, both have a direct bearing on the resolution and accuracy of the measurement. Commercial bridges are available with high specification, and are likely to be suitable for many applications. The performance achieved may in practice be limited by the connecting lines and the use of an internal reference capacitor.

## 6. Uncertainties

The standard uncertainty in the PLTS-2000 in thermodynamic terms was estimated in [Rusby *et al.* 2002] to be 0.5 mK down to 0.5 K, decreasing linearly to 0.2 mK at 0.1 K. It decreases further with falling temperature, but in percentage terms it increases to 0.3 % of  $T$  at 25 mK and about 2 % of  $T$  at 0.9 mK.

The components of uncertainty in a realization of the PLTS-2000 are due to the  $^3\text{He}$  sample purity, the thermal conditions and the measurement of pressure and capacitance. Other uncertainties will be associated with measurements of the devices and thermometers under calibration.

The sample, as supplied, should contain no more than 1 part in  $10^5$  of  $^4\text{He}$ . In that case, if there is no additional contamination from  $^4\text{He}$  in the system, the effects on the melting curve will be very small. Moreover, as Bremer [1992] points out,  $^4\text{He}$  is expected to be preferentially adsorbed on the walls of the cell, or on the sinter, and below 50 mK the impurity effect should be unobservable as the solubility of  $^4\text{He}$  in liquid or solid  $^3\text{He}$  is less than 1 ppm. On the other hand, investigations of the melting pressure of  $^3\text{He}$  contaminated with 2.1 % of  $^4\text{He}$  [Ganshin *et al.* 2001] showed that the melting-pressure minimum was depressed by about 10 kPa and shifted 18 mK to higher temperatures. There was also a change in the slope of the melting curve above and below the minimum, and the results obtained on cooling differed appreciably from warming because the melting pressure in a solution does not coincide with the freezing pressure. The relative temperature errors are larger at lower temperatures, and were as much as 15 % ( $\sim 10$  mK) at 60 mK.

At lower concentrations, Schuster *et al.* [1990] reported no change in the temperature of the minimum within  $\pm 0.3$  mK, for 0.1 % of  $^4\text{He}$  in  $^3\text{He}$ , but Bremer estimates, from considering the entropy of mixing, that for 10 ppm of  $^4\text{He}$  the melting pressure will decrease by about 0.03 kPa at 0.4 K (equivalent to about 0.06 mK or 0.015 % of  $T$ ), and that the pressure and temperature of the minimum will shift by about  $-2$  kPa and  $+0.9$  mK for 0.1 % of  $^4\text{He}$  in  $^3\text{He}$ . The temperature effect is consistent with the results of Ganshin *et al.* [2001], but the pressure effect is larger.

Although  $^4\text{He}$  impurity in small amounts is expected to be adsorbed at low temperatures, the impurity effect in the calibration of the transducer at the minimum leads to measurement uncertainties at lower temperatures. However, calibration of the transducer at a low-temperature feature pressure, if achievable, will limit this uncertainty.

The thermal contact between the sample and the experimental platform must be sufficiently good that no significant temperature gradients arise and to ensure that the thermometer responds fast enough to temperature changes. The use of sintered silver powder in the cell and metal-to-metal contact with the experimental platform, preferably gold plated, should ensure that the cell tracks the platform temperature if the measurement dissipation is not excessive. This can be investigated experimentally.

**Table 2.** Uncertainty budget for the realization of the PLTS-2000 at PTB, with values in mK. MPS stands for melting-pressure sensor

Temperature / K	0.001	0.015	0.25	0.65	1
Uncertainty components Type B	Source of uncertainty				

Temperature / K		0.001	0.015	0.25	0.65	1
$u(\delta C_1)$	Correction for the nonlinearity of the MPS	0.001	0.003	0.021	0.006	0.004
$u(\delta C_2)$	Mechanical stability of the MPS	0.001	0.004	0.032	0.009	0.006
$u(\delta C_3)$	Pressure calibration at the fixed points	0.001	0.001	0.021	0.010	0.011
$u(\delta C_4)$	Calibration against the quartz-oscillator pressure transducer and pressure balance	0.001	0.006	0.043	0.014	0.011
$u(\delta C_5)$	Instability of pressure control during calibration	0.001	0.003	0.021	0.006	0.004
$u(\delta C_6)$	Change of the head correction by temperature variation during calibration	0.001	0.001	0.004	0.001	0.001
$u(\delta C_7)$	Heating of the MPS by the excitation voltage	0.001	0.015	0.015	0.015	0.015
$u(\delta C_8)$	Temperature dependence of the dielectric susceptibility of the epoxy of the MPS	0.001	0.005	0.042	0.012	0.007
$u(\delta C_9)$	Capacitance bridge	0.003	0.003	0.021	0.006	0.004
$u(\delta C_{10})$	Temperature dependence of the pressure calibration	0.001	0.005	0.042	0.012	0.011
$u(\delta C_{11})$	$^4\text{He}$ impurities	0.010	0.010	0.010	0.010	0.010
$u(\delta T_1)$	Temperature differences between the experiment platform and the temperature sensor	0.005	0.005	0.005	0.005	0.005
$u(\delta T_2)$	Drift correction	0.005	0.005	0.005	0.005	0.005
$u(\delta T_3)$	Temperature differences between the experiment platform and the MPS	0.005	0.005	0.005	0.005	0.005
$u(\delta T_4)$	Temperature differences in the experiment platform	0.005	0.005	0.005	0.005	0.005
<b>Type B components 1 to 10 combined</b>		<b>0.005</b>	<b>0.019</b>	<b>0.092</b>	<b>0.032</b>	<b>0.027</b>
<b>Type B components all combined</b>		<b>0.015</b>	<b>0.023</b>	<b>0.093</b>	<b>0.035</b>	<b>0.030</b>
<b>Type A uncertainty component</b>		<b>0.005</b>	<b>0.005</b>	<b>0.005</b>	<b>0.005</b>	<b>0.005</b>
<b>Combined standard uncertainty (k = 1)</b>		<b>0.016</b>	<b>0.024</b>	<b>0.093</b>	<b>0.036</b>	<b>0.031</b>
<b>Expanded uncertainty (k = 2)</b>		<b>0.031</b>	<b>0.048</b>	<b>0.186</b>	<b>0.071</b>	<b>0.061</b>

Many aspects of the pressure measurement have already been covered. With careful design and a good measuring system, the pressure sensitivity of the transducer can be about 1 part in  $10^6$ , and the calibration can give an uncertainty of about  $\pm 50$  Pa (SHH, CFS). To achieve overall uncertainties of this order also requires proper estimation of the hydrostatic pressure head. The uncertainty of using a secondary gauge depends on the uncertainty of its calibration

and on its stability, and is unlikely to be better than  $\pm 100$  Pa. As was discussed in the previous section, an absolute calibration of the transducer is not needed if it is normalized against the  $^3\text{He}$  features, as specified in the PLTS-2000, and there is also no need to correct for the hydrostatic pressure head effect. Only the linearity, hysteresis and reproducibility remain, and the resulting pressure uncertainties can be of the order of  $\pm 10$  Pa.

As an example, Table 2 is the complete uncertainty budget for the realization of the PLTS-2000 over the whole range at PTB [Schuster *et al.* 1990], with values given at selected temperatures. It is based on the cell and measurement system described in SHH, and applies to the case where the transducer is calibrated against a quartz-oscillator pressure gauge which is traceable to a pressure balance. However, to conform with the PLTS-2000, the transducer calibration is normalized at the low-temperature features and at the pressure minimum, to give the required values at these points, and to obviate the need for absolute accuracy or to correct for the hydrostatic pressure effect, apart from its small temperature dependence. There are ten Type B components of uncertainty related to capacitance or pressure measurement, one for  $^3\text{He}$  purity, and four for thermal effects in the melting-pressure sensor (MPS) and the experiment platform.

## 7. Relationship with the ITS-90

In the range 0.65 K to 1 K the PLTS-2000 overlaps the ITS-90 and there is the potential for non-uniqueness between the two scales; that is, between the equation for  $^3\text{He}$  vapour pressures specified in the ITS-90 and that for  $^3\text{He}$  melting pressures in the PLTS-2000. In fact it has for some time been suspected that the ITS-90 vapour-pressure equation deviates from thermodynamic temperature below 1 K [Fogle *et al.* 1992, Schuster and Hechtfisher 1992, Fellmuth and Schuster 1992]. In this region the PLTS-2000 melting pressure equation was derived from CMN magnetic thermometry at NIST and PTB, linked to the ITS-90 in the range above 1.2 K and supported by noise thermometry at both institutes, and therefore it would not be affected by errors in the ITS-90 at lower temperatures.

Comparisons of  $^3\text{He}$  vapour pressures and melting pressures have now been performed at PTB [Engert *et al.* 2007], and Figure 10 shows that the differences between the two scales rise from about 0.6 mK at 1 K to 1.5 mK at 0.65 K. The uncertainties, plotted at  $k = 1$ , are those in the comparisons, see Table 5 of Reference 35, and do not include the thermodynamic uncertainties of the PLTS-2000.

In view of these differences, it is recommended that the melting pressure (PLTS-2000) should be used for preference, on the grounds both of better thermodynamic accuracy and the potential for lower uncertainty of realization. Where it is desired to use vapour pressures, the new more accurate equations of [Engert *et al.* 2007] are now available as alternatives to the equation specified in the ITS-90.

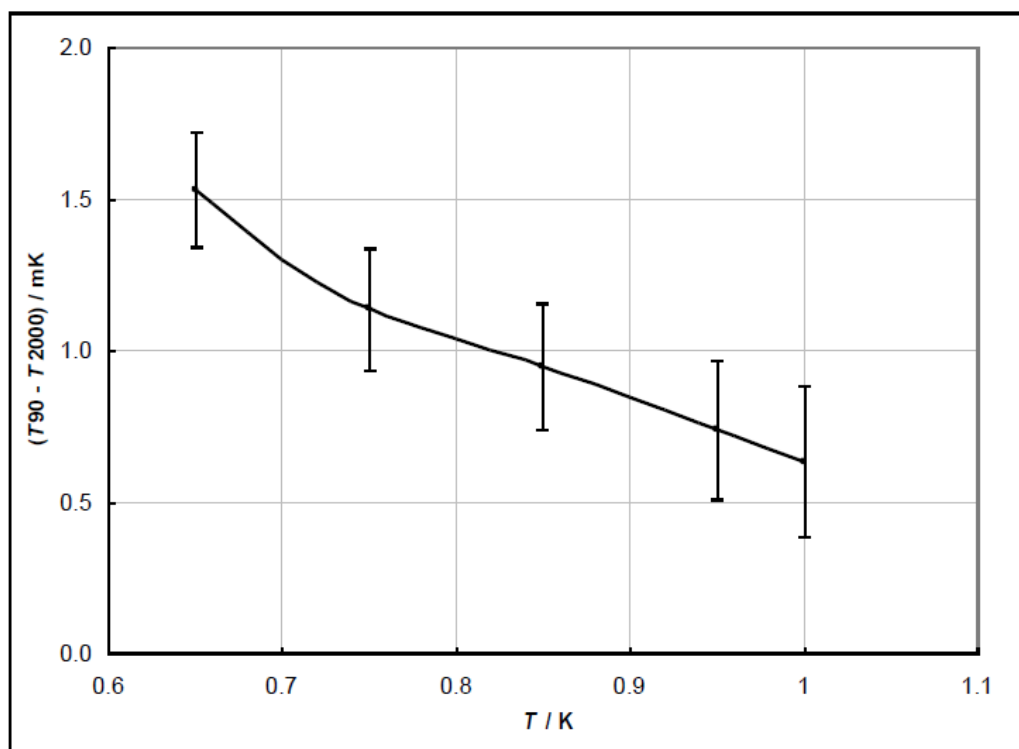


**Figure 10 — Differences ( $T_{90} - T_{2000}$ ) obtained at PTB from comparisons of  $^3\text{He}$  vapour pressures and melting pressures, using rhodium-iron resistance thermometers as intermediaries [Engert *et al.* 2007]. Uncertainty bars for the scale comparisons are shown at  $k = 1$ .**



## Annex 1. Tables of melting pressures and temperatures

**Table A1.1.** Values of melting pressure,  $p_m$ /MPa, and  $dp_m/dT_{2000}$  in MPaK<sup>-1</sup>, at intervals of 0.1 mK up to 2.9 mK.

$T_{2000}$ / mK	0.0	0.1	0.2	0.3	0.4	0.5	0.6	0.7	0.8	0.9
1	3.439068	3.438768	3.438457	3.438135	3.437806	3.437470	3.437128	3.436782	3.436430	3.436074
	-	-	-	-	-	-	-	-	-	-
	2.89860	3.06549	3.17469	3.25711	3.32587	3.38665	3.44196	3.49297	3.54023	3.58409
2	3.435714	3.435348	3.434981	3.434610	3.434235	3.433858	3.433478	3.433096	3.432711	3.432324
	-	-	-	-	-	-	-	-	-	-
	3.62477	3.66246	3.69736	3.72964	3.75948	3.78705	3.81252	3.83603	3.85775	3.87781

**Table A1.2.** Values of melting pressure,  $p_m$ /MPa, and  $dp_m/dT_{2000}$  in MPaK<sup>-1</sup>, at intervals of 1 mK up to 109 mK.

$T_{2000}$ / mK	0	1	2	3	4	5	6	7	8	9
0	3.439068	3.435714	3.431935	3.427970	3.423919	3.419831	3.415732	3.411634	3.407546	
	-	-	-	-	-	-	-	-	-	-
	2.89860	3.62477	3.89634	4.01944	4.07464	4.09644	4.10031	4.09380	4.08094	
10	3.403473	3.399419	3.395385	3.391374	3.387385	3.383421	3.379481	3.375566	3.371676	3.367811
	-	-	-	-	-	-	-	-	-	-
	4.06402	4.04439	4.02293	4.00020	3.97657	3.95232	3.92763	3.90263	3.87743	3.85209
20	3.363971	3.360157	3.356368	3.352606	3.348868	3.345155	3.341468	3.337806	3.334169	3.330557
	-	-	-	-	-	-	-	-	-	-
	3.82669	3.80126	3.77584	3.75046	3.72513	3.69987	3.67470	3.64963	3.62467	3.59982
30	3.326968	3.323406	3.319868	3.316354	3.312865	3.309398	3.305958	3.302540	3.299147	3.295776
	-	-	-	-	-	-	-	-	-	-
	3.57509	3.55048	3.52601	3.50167	3.47746	3.45339	3.42945	3.40566	3.38201	3.35849
40	3.292430	3.289106	3.285806	3.282528	3.279274	3.276042	3.272833	3.269647	3.266482	3.263340
	-	-	-	-	-	-	-	-	-	-
	3.33512	3.31189	3.28880	3.26585	3.24304	3.22038	3.19785	3.17546	3.15321	3.13111
50	3.260220	3.257122	3.254045	3.250990	3.247957	3.244945	3.241954	3.238985	3.236036	3.233108
	-	-	-	-	-	-	-	-	-	-
	3.10913	3.08730	3.06560	3.04404	3.02261	3.00132	2.98016	2.95913	2.93824	2.91747
60	3.230201	3.227315	3.224448	3.221603	3.218777	3.215971	3.213186	3.210420	3.207674	3.204947
	-	-	-	-	-	-	-	-	-	-
	2.89684	2.87633	2.85595	2.83570	2.81558	2.79558	2.77570	2.75595	2.73632	2.71681
70	3.202240	3.199552	3.196884	3.194234	3.191604	3.188992	3.186398	3.183825	3.181268	3.178732

$T_{2000}$ / mK	0	1	2	3	4	5	6	7	8	9
80	-	-	-	-	-	-	-	-	-	-
	2.69743	2.67816	2.65901	2.63998	2.62106	2.60227	2.58358	2.56501	2.54656	2.52821
	3.176213	3.173713	3.171223	3.168764	3.166317	3.163883	3.161476	3.159082	3.156703	3.154346
90	-	-	-	-	-	-	-	-	-	-
	2.50998	2.49186	2.47385	2.45595	2.43816	2.42047	2.40289	2.38541	2.36804	2.35077
	3.152004	3.149673	3.147373	3.145073	3.142803	3.140547	3.138306	3.136082	3.133874	3.131682
100	-	-	-	-	-	-	-	-	-	-
	2.33361	2.31655	2.29959	2.28273	2.26597	2.24930	2.23274	2.21627	2.19990	2.18363
	3.129507	3.127347	3.125204	3.123076	3.120963	3.118863	3.116783	3.114724	3.112673	3.110642
	-	-	-	-	-	-	-	-	-	-
	2.16745	2.15136	2.13537	2.11947	2.10366	2.08794	2.07231	2.05677	2.04132	2.02596

**Table A1.3.** Values of melting pressure,  $p_m$ /MPa, and  $dp_m/dT_{2000}$  in MPaK<sup>-1</sup>, at intervals of 10 mK from 0.1 K to 1 K.

[illegible]

## References

- [1] Adams E D 1993 High-resolution capacitive pressure gauges *Rev. Sci. Instrum.* **64** 601-611
- [2] Adams E D 2005 *Progress in Low Temperature Physics* Vol. 15, Chapter 4, edited by W Halperin, Elsevier B. V. See also *Temperature, its Measurement and Control in Science and Industry*, 2003 vol. 7 (edited by D C Ripple), AIP Conference Proceedings, Melville, New York, pp. 107-112
- [3] Betts D S 1976 *Refrigeration and Thermometry below 1 K*, Sussex University Press
- [4] Bittner D N and Adams E D 1994 Solidification of helium in confined geometries *J. Low Temp. Phys.* **97** 519-535
- [5] Bogayavlenskii I V, Karnatsevich L V and Konareva V G 1978 *Soviet J. Low Temp. Phys.* **4** (5) 265
- [6] Bremer J 1992 *Noise Thermometry and the  $^3\text{He}$  Melting Curve below 1 K*, Thesis, Leiden University
- [7] Bremer J and Durieux M 1992 *Temperature, its Measurement and Control in Science and Industry* vol. 6 (edited by J. F. Schooley), American Institute of Physics, New York, pp. 15-20
- [8] Colwell J H, Fogle W E and Soulen R J 1992 *Temperature, its Measurement and Control in Science and Industry*, vol. 6 (edited by J. F. Schooley), American Institute of Physics, New York, pp. 101-106
- [9] Durieux M and Reesink A L 1999 7<sup>th</sup> International Symposium on *Temperature and Thermal Measurements in Industry and Science*, edited by J. Dubbeldam and M. deGroot pp. 19-26
- [10] Engert J, Fellmuth B and Jousten K 2002 A new  $^3\text{He}$  vapour-pressure based temperature scale from 0.65K to 3.2K consistent with the PLTS-2000 *Metrologia* **44** 40-52
- [11] Engert J, Fellmuth B and Hoffmann A 2003 2<sup>nd</sup> International Symposium on *Low temperature Thermometry*, Wrocław, pp. 13-18, and Document CCT/03-09, [www.bipm.org](http://www.bipm.org), BIPM
- [12] Fellmuth B and Schuster G 1992 Thermodynamic Inconsistency of the ITS-90 Below 1.5 K *Metrologia* **29** 415-423
- [13] Fellmuth B, Hechtfisher D and Hoffmann A 2003 *Temperature, its Measurement and Control in Science and Industry*, vol. 7 (edited by D C Ripple), AIP Conference Proceedings, Melville, New York, pp. 71-76
- [14] Fogle W E, Soulen R J and Colwell J H 1992 *Temperature, its Measurement and Control in Science and Industry*, vol. 6 (edited by J F Schooley), American Institute of Physics, New York, pp. 85-90

- [15] Ganshin A N, Grigor'ev V N, Maidanov V A, Penzev A, Rudavskii E, Rybalko A and Syrnikov E V 2001 On the influence of low  $^4\text{He}$  impurity content on the melting curve of  $^3\text{He}$  *Low Temperature Physics (Russia)* **27** N6 509-510
- [16] Greywall D S and Busch P A 1982  $^3\text{He}$ -melting-curve thermometry *J. Low Temp. Phys.* **46** 451-465
- [17] Hudson R P, Marshak H, Soulen R J and Utton D B 1975 Recent advances in thermometry below 300 mK *J. Low Temp. Phys.* **20** 1-103
- [18] Ihas G G and Pobell F 1974 Correlation length, finite-geometry effects, and universality in pressurized superfluid helium near  $T_\lambda$  *Phys. Rev. A* **9** 1278-1296
- [19] Jarvis J F, Ramm D and Meyer H 1968 Measurement of  $(\rho/\rho_0)$  and Related Properties in Solidified Gases. I. Solid  $\text{He}^4$  *Phys. Rev.* **170** 320-327
- [20] Lounasmaa O V 1974 *Experimental Principles and Methods below 1 K*, Academic Press
- [21] Mikheev V A, Masuhara M, Wagner T, Eska G, Mohandas P and Saunders J 1994 Cylindrical pressure gauge *Cryogenics* **34** 167-168.
- [22] Pitre L, Hermier Y and Bonnier G 2003 *Temperature, its Measurement and Control in Science and Industry*, vol 7 (edited by D C Ripple), AIP Conference Proceedings, Melville, New York, pp. 95-100
- [23] Pobell F 1996 *Matter and Methods at Low Temperatures*, Springer Verlag, 2nd Edition.
- [24] Richardson R C and Smith E N 1988 *Experimental Techniques in Condensed Matter, Physics at Low Temperatures*, Addison-Wesley
- [25] Rusby R L, Durieux M, Reesink A L, Hudson R P, Schuster G, Kühne M, Fogle W E, Soulen R J and Adams E D 2002 The Provisional Low Temperature Scale from 0.9 mK to 1 K, PLTS-2000 *J. Low Temp. Physics* **126** 633-642. See also *Temperature, its Measurement and Control in Science and Industry* 2003 vol. 7 (edited by D C Ripple), AIP Conference Proceedings, Melville, New York, pp. 77-82
- [26] Rusby R L, Fellmuth B, Engert J, Fogle W E, Adams E D, Pitre L and Durieux M 2007 Realization of the  $^3\text{He}$  Melting Pressure Scale, PLTS-2000 *J. Low Temp. Physics* **149** 156-175
- [27] Scribner R A and Adams E D 1970 Use of the  $^3\text{He}$  Melting Curve for Low Temperature Thermometry *Rev. Sci. Instrum.* **41** 287-288
- [28] Schuster G and Wolber L 1986 Automated  $^3\text{He}$  melting curve thermometer *J. Phys. E: Sci. Instrum.* **19** 701-705
- [29] Schuster G, Hechtfischer D, Buck W and Hoffmann A 1990 *Proceedings of the 19th International Conference on Low Temperature Physics*, Physica B165 & 166 pp. 31-32

- [30] Schuster G and Hechtfischer D 1992 *Temperature, its Measurement and Control in Science and Industry* vol. 6 (edited by J F Schooley), American Institute of Physics, New York, pp. 97-100
- [31] Schuster G, Hechtfischer D and Fellmuth B 1994 Thermometry below 1 K *Rep. Prog. Phys.* **57** 187-230
- [32] Schuster G, Hoffmann A and Hechtfischer D 2001 *Realisation of the temperature scale PLTS-2000 at PTB*, PTB, Braunschweig, PTB-ThEx-21, 29pp, available through [www.ptb.de](http://www.ptb.de).
- [33] Straty G C and Adams E D 1969 Highly Sensitive Capacitive Pressure Gauge *Rev. Sci. Instrum.* **40** 1393-1397
- [34] Van Degriift C T 1975 Tunnel diode oscillator for 0.001 ppm measurements at low temperatures *Rev. Sci. Instrum.* **46** 599-607
- [35] Wilks J 1967 *Liquid and Solid Helium*, Clarendon Press, Oxford. See also Sherman R H and Edeskuty F J 1960 *Ann. Phys.* **9** 522, and Grilly E R and Hammel E F 1961 *Prog. Low Temp. Phys.* **3**, ed Gorter, North Holland, p. 122